Magnetodielectric coupling in core/shell Ba Ti O 3/γ - Fe 2 O 3 nanoparticles

Y. S. Koo, T. Bonaedy, K. D. Sung, J. H. Jung, J. B. Yoon, Y. H. Jo, M. H. Jung, H. J. Lee, T. Y. Koo, and Y. H. Jeong

Citation: Applied Physics Letters **91**, 212903 (2007); doi: 10.1063/1.2817940
View online: http://dx.doi.org/10.1063/1.2817940
View Table of Contents: http://scitation.aip.org/content/aip/journal/apl/91/21?ver=pdfcov
Published by the AIP Publishing

Magnetodielectric coupling in core/shell $BaTiO_3/\gamma$-Fe_2O_3 nanoparticles

Y. S. Koo, T. Bonaedy, K. D. Sung, and J. H. Jung[a)]
Department of Physics, Inha University, Incheon 402-751, Korea

J. B. Yoon, Y. H. Jo, and M. H. Jung
Quantum Material Research Team, Korea Basic Science Institute, Daejeon 305-333, Korea

H. J. Lee, T. Y. Koo, and Y. H. Jeong
Department of Physics and Pohang Accelerator Lab., Pohang University of Science and Technology, Pohang 790-784, Korea

(Received 18 September 2007; accepted 6 November 2007; published online 20 November 2007)

We report an intriguing magnetodielectric coupling in $BaTiO_3/\gamma$-Fe_2O_3 dielectric core/ferrimagnetic shell nanoparticles. The dielectric constant steeply increases with magnetic field, and the frequency dependent magnetodielectric curve shows a resonancelike peak at high temperatures, while it decreases smoothly with field and no peak appears in the frequency dependent magnetodielectric curve at low temperatures. We attribute the observed magnetodielectric coupling to the Maxwell-Wagner effect combined with magnetoresistance at high temperatures and to possible spin-lattice coupling and its modification near interfaces at low temperatures. © *2007 American Institute of Physics*. [DOI: 10.1063/1.2817940]

The prospects of the magnetic control of electrical properties of a material, such as polarization and dielectric constant, or vice versa have given rise to active researches.[1,2] However, due to the scarcity of single-phase materials as well as the low temperature nature of magnetoelectric and magnetodielectric effects, lots of researches have concentrated on two-phase materials, such as heterostructure thin films and composites.[3,4] Especially, Zheng *et al.*[3] reported the change of magnetization near the ferroelectric transition temperature in nanopillar $CoFe_2O_4$ embedded $BaTiO_3$ thin film, where strain at the interface is quite important. In this regard, core/shell-type nanoparticles may possess a strong coupling between electricity and magnetism, and thus offer a route to multifunctionality.[5] Since the core and shell combination can be composed of a various sets of piezoelectric and magnetoresistive materials with high transition temperatures, core/shell nanoparticles with a controlled interface may give rise to intriguing magnetoelectric[6] and/or magnetodielectric effects. Untill now, however, there are few works on magnetodielectric property for electric/magnetic core/shell nanoparticles. Note that there were two reports on magnetodielectric property in ferrite nanoparticles,[7,8] but none were core/shell structures.

In this letter, we report a systematic investigation on magnetic and magnetodielectric properties of $BaTiO_3/\gamma$-Fe_2O_3 core/shell nanoparticles with controlled shell thickness. Possibly due to the strain and/or the formation of antiferromagnetic antiphase boundary near core/shell interface, the magnetic structure of shell might be modified; which results in the change of coercive field as well as the changes of magnitude and behavior of magnetodielectric coupling. In addition, the sign and magnitude of magnetodielectric property are significantly changed depending on temperature and shell thickness, respectively. These results may imply that electric/magnetic core/shell nanoparticles could be potentially useful for tunable magnetodielectric devices.

Core/shell-type $BaTiO_3/\gamma$-Fe_2O_3 nanoparticles were synthesized by a sonochemical method with controlled reaction time. Commercial $BaTiO_3$ nanoparticles were thoroughly dispersed in a reaction vessel, which was kept at 70 °C. By using a peristaltic pump, the volume ratio of reaction solutions ($FeCl_2$ and CH_3COOH) and oxidation solutions (NH_4OH and $NaNO_2$) was kept constant (~2 ml/min) and ultrasonic waves (10 kHz, 700 W) were applied with varying time from 1 to 4 h. The obtained powders were fired at 300 °C for 4 h in air to obtain uniform γ-Fe_2O_3 phase in shell.

The core/shell structure and particle size were examined by a field-effect scanning/transmission electron microscope and a dynamic light scattering analyzer, respectively. Magnetic and dielectric properties of nanoparticles were measured by a superconducting quantum interference device and an *LCR* meter, respectively. For dielectric measurement, the powders were isostatically pressed (~200 MPa) into a disk shape ($\varphi 7 \times 1$ mm^2) and then fired at 300 °C, i.e., the same temperature as nanoparticle synthesis. The final density of pellets was estimated to be ~4.6 g/cm^3 (~80% of their theoretical value), which was dense enough for preventing percolation of electrode. The pellets were deposited with silver paint on opposite sides to make a parallel plate capacitor. For magnetodielectric measurement, we applied external magnetic field by a superconducting magnet, parallel to the electric field used for dielectric measurement, i.e., $H \| E$.

Scanning electron microscope (SEM) measurement clearly reveals the $BaTiO_3/\gamma$-Fe_2O_3 core/shell structure and the increase of shell thickness with reaction time. Figure 1 shows the SEM images of $BaTiO_3$ [Fig. 1(a)] and $BaTiO_3/\gamma$-Fe_2O_3 with successive reaction times from 1 to 4 h [Figs. 1(b)–1(e)]. With increasing reaction time, the surface of spherical $BaTiO_3$ becomes somewhat irregular and larger due to the coated γ-Fe_2O_3, hence forming $BaTiO_3/\gamma$-Fe_2O_3 core/shell particles. In the insets of Figs. 1(a)–1(e), we show the distribution of particle size and log-normal functional fitting (solid lines). Based on fitting results and the size of $BaTiO_3$ ($\varphi \sim 70$ nm), we estimate the

a)Author to whom correspondence should be addressed. Electronic mail: jbjung@inha.ac.kr

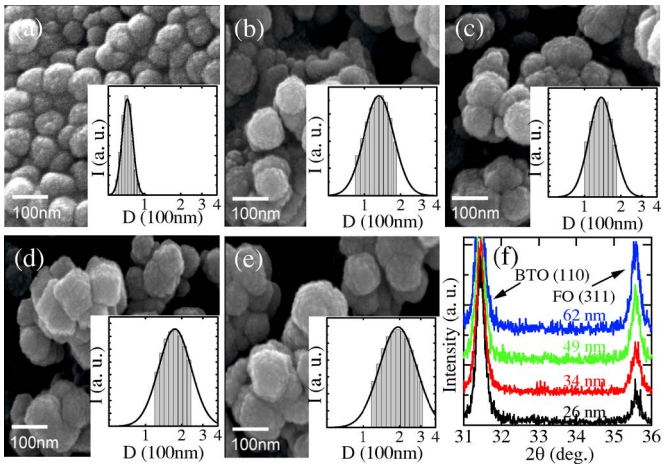

FIG. 1. (Color online) SEM images of (a) BTO and BTO/FO with different shell thicknesses [(b)–(e)]. For each image, the distribution of particle sizes and log-normal fitting curves are shown. (f) Normalized x-ray diffraction patterns near BTO (110) and FO (311) peaks.

thicknessess of γ-Fe_2O_3 as 26, 34, 49, and 62 nm for 1, 2, 3, and 4 h reaction times, respectively. Hereafter, we call $BaTiO_3$/ γ-Fe_2O_3 with different shell thicknesses as BTO/FO (thickness of shell).

The grain size of FO seems to be nearly the same irrespective of shell thickness. In Fig. 1(f), we show the x-ray diffraction patterns for selected angles. We normalized the (110) peak intensity of BTO and compared the (311) peak of FO. Though the (311) peak intensity systematically increases with the thickness of FO, the full width at half maximum is nearly the same. By using Scherrer's formula and independent transmission electron microscope measurement, we estimate the grain size as ~25 nm. These results suggest that nearly the same grain size of FO is plated on BTO with different thicknesses.

Magnetic susceptibility measurement reveals that all BTO/FO nanoparticles lie in their blocked states. As representatives, we show zero field cooled (ZFC) and field cooled (FC) magnetic susceptibilities for BTO/FO (26 nm) in Fig. 2(a). One may clearly notice an irreversible magnetic susceptibility even at 350 K, i.e., the maximum temperature

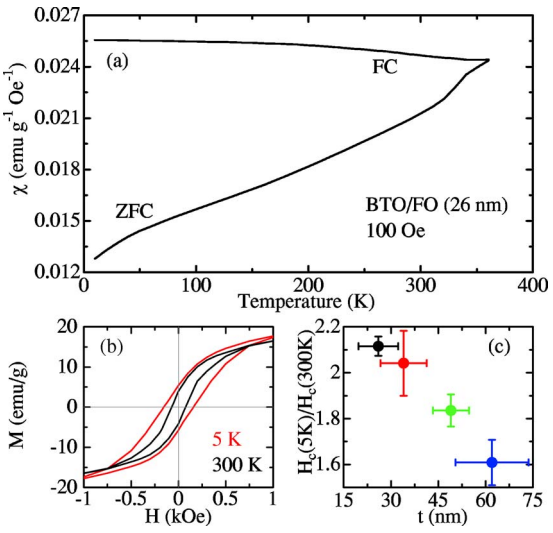

FIG. 2. (Color online) (a) ZFC and FC magnetic susceptibilities and (b) magnetic hysteresis loops at 5 and 300 K for BTO/FO (26 nm). (c) Shell thickness dependent normalized coercive field, i.e., $H_C(5\text{ K})/H_C(300\text{ K})$.

of our measurement. The irreversible behaviors have frequently been observed in magnetic nanoparticles in their blocked states. The blocking temperature T_B, where the ZFC susceptibility is maximized, has been referred as a crossover from the high temperature superparamagnetic state to the low temperature blocked state. Recently, Park *et al.*[9] reported the systematic increase of T_B with the crystal size in FO nanoparticles. Since the crystalline size of our FO is ~25 nm and the magnetic dipole interaction might increase due to dense FO,[10] we believe that the T_B of our BTO/FO can reach ~350 K. Hence, the nanoparticles show clear hysteresis loops at 300 and 5 K [see, Fig. 2(b)].

The core BTO seems to affect the magnetic properties of shell FO through the strain and/or the formation of antiferromagnetic antiphase boundary in FO due to the lattice mismatch between core (3.994 Å) and shell (8.355 Å). In Fig. 2(c), we show the thickness dependence of the normalized coercive fields, i.e., $H_C(5\text{ K})/H_C(300\text{ K})$. Clearly, the $H_C(5\text{ K})/H_C(300\text{ K})$ linearly decreases with increasing thickness. Specifically, the value of $H_C(5\text{ K})$ [$H_C(300\text{ K})$] for BTO/FO (62 nm) is 141 Oe (87 Oe) and that for BTO/FO (26 nm) is 171 Oe (81 Oe), which may imply that the change of $H_C(5\text{ K})/H_C(300\text{ K})$ is not mainly due to a demagnetization field. Instead, the change of $H_C(5\text{ K})/H_C(300\text{ K})$ with thickness might be related with the magnetocrystalline anisotropy due to the strain and/or the formation of antiferromagnetism in FO due to antiphase boundary. Note that the formation of antiferromagnetic antiphase boundary has frequently been observed and known to affect the magnetotransport property in ferrite thin films,[11] not single crystal, on substrate with large lattice mismatch, as similar to our core/shell nanoparticles. With the increase of shell thickness, the strain and/or mismatch will be relaxed; hence, the coercive field ratio decreases as consistent with our results.

BTO/FO nanoparticles show intriguing magnetodielectric (MD) coupling, depending on temperature as well as shell thickness. Figure 3(a) shows the MD curves $\Delta\varepsilon_1/\varepsilon_1$ $(=[\varepsilon_1(H)-\varepsilon_1(0\text{ T})]/\varepsilon_1(0\text{ T}))$ of BTO/FO (62 nm) at 300 kHz for selected temperatures. Clearly, dielectric constant significantly changes upon external magnetic field. Interestingly, the dielectric constant at low temperatures, such as 20 K, decreases with magnetic field, while that at high temperatures, such as 200 K, increases with magnetic field. In the low magnetic field region, especially below 2 T, the dielectric constant at 20 K smoothly decreases, while that at 200 K sharply increases. Irrespective of shell thickness, as shown in Fig. 3(b), the sign of MD coefficient is negative at low temperature and positive at high temperature, and the sign change seems to occur near 60 K. Also the temperature variations of MD effect become more significant as the thickness of shell increases.

To address the origin of MD coupling at high temperature, e.g., 200 K, we show the frequency dependent $\Delta\varepsilon_1/\varepsilon_1$ at 1, 3, 5, and 7 T for BTO/FO (62 nm) in Fig. 3(c). Clearly, $\Delta\varepsilon_1/\varepsilon_1$ curve shows strong frequency dependence with a resonancelike peak. With increasing magnetic field, the peak becomes broader and the peak position (solid circles) seems to move to the higher frequency.

The observed positive MD effect at high temperature could be explained based on the combination of Maxwell-Wagner effect and negative magnetoresistance. Recently,

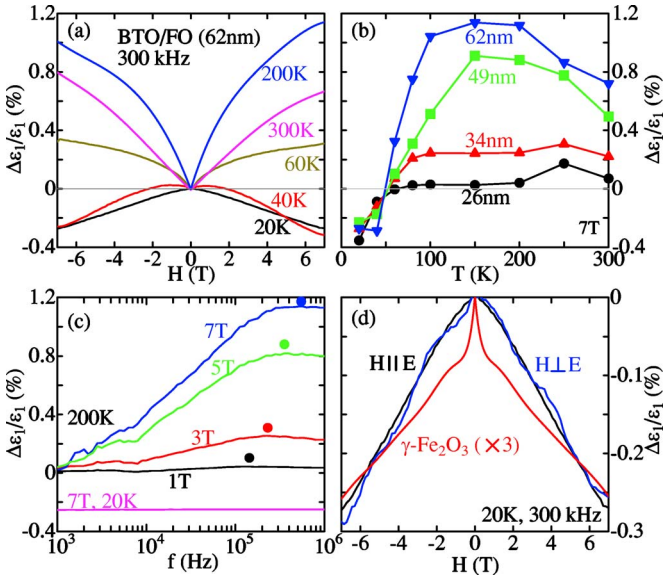

FIG. 3. (Color online) (a) MD curves of BTO/FO (62 nm) at 300 kHz. (b) Temperature dependent MD values at 7 T for BTO/FO. (c) Frequency dependent MD curves at 200 and 20 K. Solid circles represent the frequencies of maximum MD value. (d) MD curves of BTO/FO (62 nm) for $H \| E$ (a black line) and $H \perp E$ (a blue line) and that of FO (a red line) at 20 K. For clarity, we have multiplied three for the MD curve of FO.

Catalan reported that the MD effect can show up due to magnetoresistance, without magnetoelectric coupling, in heterogeneous samples.[12] According to this model, the MD curve should show a resonancelike peak due to the conductivity cutoff of charge carrier, i.e., the frequency dependent MD curve should be maximized when the measured frequency nearly coincides with $1/RC$, where R and C represent the resistance and capacitance, respectively.[13] Since the resistivity of FO decreases with magnetic field, i.e., negative magnetoresistance,[13] the frequency for maximum MD effect should move to a higher frequency and the MD curve should be broader, as consistent with our observation. Therefore, it is quite reasonable to attribute the high temperature MD effect to extrinsic resistive origin.

Observed MD effect at low temperature, e.g., 20 K, might not be originated from (tunneling) magnetoresistance, since the resistivities of both BTO and FO, hence BTO/FO nanoparticle, are very high ($>10^9 \Omega$ cm). As consistent, the frequency dependence of $\Delta\varepsilon_1/\varepsilon_1$ at 7 T does not show any peak, but becomes negatively flat for all measured frequencies [Fig. 3(c)]. To see the possibility of magnetostriction effect of our BTO/FO, we also measured the MD curves for $H \| E$ (a black line) and for $H \perp E$ (a blue line) at 20 K [see Fig. 3(d)]. However, the experimental data are nearly the same within error bar suggesting the negligible effect of magnetostriction on the MD effect.

To address the possible origin of negative MD coupling at 20 K, we compare the MD curves of BTO/FO (62 nm) and FO (a red line) in Fig. 3(d). Although the signal is quite weak, the FO itself clearly shows the MD effect with negative sign. However, the $\Delta\varepsilon_1/\varepsilon_1$ value of FO is approximately three times smaller than that of BTO/FO (62 nm). Although the exact origin of MD effect at low temperature is unclear, the enhanced MD effect of BTO/FOas compared with that of FO might suggest that the spin coupled with lattice, which can be affected by strain, may be responsible for negative MD effect at low temperature, as frequently observed in intrinsic multiferroics, such as $BiMnO_3$.[14]

The formation of antiferromagnetic antiphase boundary in FO seems to affect the shape of the MD curve at the low magnetic field region. As shown clearly in Fig. 3(d), the MD curve of BTO/FO (62 nm) smoothly decreases while that of FO steeply decreases below 2 T (at high magnetic field, e.g., 7 T, the curvatures of MD curves become similar). Note here that the smooth curvature of MD curve has been observed in antiferromagnetic $TeCuO_3$.[15] Therefore, we speculate that the antiferromagnetic spin texture in FO near BTO/FO interface may affect the MD property at 20 K for the low magnetic field region.

In summary, we have investigated the magnetodielectric coupling in $BaTiO_3/\gamma$-Fe_2O_3 core/shell nanoparticles. The changes in sign and magnitude of the magnetodielectric coupling turned out to depend sensitively on temperature, shell thickness, and strain/mismatch near interfaces; this in turn suggests that the electric/magnetic core/shell nanoparticles could be tailored and thus be useful for tunable magnetodielectric devices.

This work was supported by the Korea Research Foundation Grant funded by the Korean Government (MOEHRD) (KRF-2005-070-C00053) and (KRF-2005-041-C00164), and the SRC project of MOST/KOSEF. This work was supported by Cooperative Research Program of the KRCF and National Research Program of the MOCIE to M.H.J.

[1] T. Kimura, T. Goto, H. Shintani, K. Ishizaka, T. Arima, and Y. Tokura, Nature (London) **426**, 55 (2003).
[2] N. Hur, S. Park, P. A. Sharma, J. S. Ahn, S. Guha, and S.-W. Cheong, Nature (London) **429**, 392 (2004).
[3] H. Zheng, J. Wang, S. E. Lofland, Z. Ma, L. Mohaddes-Ardabili, T. Zhao, L. Salamanca-Riba, S. R. Shinde, S. B. Ogale, F. Bai, D. Viehland, Y. Jia, D. G. Schlom, M. Wuttig, A. Roytburd, and R. Ramesh, Science **303**, 661 (2004).
[4] C.-W. Nan, G. Liu, Y.-H. Lin, and H. Chen, Phys. Rev. Lett. **94**, 197203 (2005).
[5] S. Mornet, C. Elissalde, O. Bidault, F. Weill, E. Sellier, O. Nguyen, and M. Maglione, Chem. Mater. **19**, 987 (2007).
[6] V. Corral-Floresa, D. Bueno-Baques, D. Carrillo-Flores, and J. A. Matutes-Aquino, J. Appl. Phys. **99**, 08J503 (2006).
[7] M. Gich, C. Frontera, A. Roig, E. Molins, J. Fontcuberta, N. Bellido, Ch. Simon, and C. Fleta, Nanotechnology **17**, 687 (2006).
[8] G. Lawes, R. Tackett, B. Adhikary, R. Naik, O. Masala, and R. Seshadri, Appl. Phys. Lett. **88**, 242903 (2006).
[9] J. Park, K. An, Y. Hwang, J.-G. Park, H.-J. Noh, J.-Y. Kim, J.-H. Park, N.-M. Hwang, and T. Hyeon, Nat. Mater. **3**, 891 (2004).
[10] J. Garcia-Otero, M. Porto, J. Rivas, and A. Bunde, Phys. Rev. Lett. **84**, 167 (2000).
[11] W. Eerenstein, T. T. M. Palstra, S. S. Saxena, and T. Hibma, Phys. Rev. Lett. **88**, 247204 (2002).
[12] G. Catalan, Appl. Phys. Lett. **88**, 102902 (2006).
[13] T. Bonaedy, Y. S. Koo, K. D. Sung, and J. H. Jung, Appl. Phys. Lett. **91**, 132901 (2007).
[14] T. Kimura, S. Kawamoto, I. Yamada, M. Azuma, M. Takano, and Y. Tokura, Phys. Rev. B **67**, 180401 (2003).
[15] G. Lawes, A. P. Ramirez, C. M. Varma, and M. A. Subramanian, Phys. Rev. Lett. **91**, 257208 (2003).